

# Projected expansion of the subtropical biome and contraction of the temperate and equatorial upwelling biomes in the North Pacific under global warming

Jeffrey J. Polovina<sup>1\*</sup>, John P. Dunne<sup>2</sup>, Phoebe A. Woodworth<sup>1</sup>, and Evan A. Howell<sup>1</sup>

<sup>1</sup>NOAA Pacific Islands Fisheries Science Center, Honolulu, HI, USA

<sup>2</sup>NOAA Geophysical Fluid Dynamics Laboratory, Princeton, NJ, USA

\*Corresponding Author: tel: +1 808 983 5390; fax: +1 808 983 2933; e-mail: [jeffrey.polovina@noaa.gov](mailto:jeffrey.polovina@noaa.gov).

Polovina, J. J., Dunne, J. P., Woodworth, P. A., and Howell, E. A. Projected expansion of the subtropical biome and contraction of the temperate and equatorial upwelling biomes in the North Pacific under global warming. – ICES Journal of Marine Science, doi:10.1093/icesjms/fsq198.

Received 3 June 2010; accepted 5 December 2010.

A climate model that includes a coupled ocean biogeochemistry model is used to define large oceanic biomes in the North Pacific Ocean and describe their changes over the 21st century in response to the IPCC Special Report on Emission Scenario A2 future atmospheric CO<sub>2</sub> emissions scenario. Driven by enhanced stratification and a northward shift in the mid-latitude westerlies under climate change, model projections demonstrated that between 2000 and 2100, the area of the subtropical biome expands by ~30% by 2100, whereas the area of temperate and equatorial upwelling (EU) biomes decreases by ~34 and 28%, respectively, by 2100. Over the century, the total biome primary production and fish catch is projected to increase by 26% in the subtropical biome and decrease by 38 and 15% in the temperate and the equatorial biomes, respectively. Although the primary production per unit area declines slightly in the subtropical and the temperate biomes, it increases 17% in the EU biome. Two areas where the subtropical biome boundary exhibits the greatest movement is in the northeast Pacific, where it moves northwards by as much as 1000 km per 100 years and at the equator in the central Pacific, where it moves eastwards by 2000 km per 100 years. Lastly, by the end of the century, there are projected to be more than 25 million km<sup>2</sup> of water with a mean sea surface temperature of 31°C in the subtropical and EU biomes, representing a new thermal habitat. The projected trends in biome carrying capacity and fish catch suggest resource managers might have to address long-term trends in fishing capacity and quota levels.

**Keywords:** biomes, climate model, global warming, North Pacific, ocean biogeochemistry model.

## Introduction

Marine ecosystems are likely to be affected by future anthropogenic climate change through a suite of changes in ocean conditions and dynamics that alter ecological processes, including primary production, species distributions, phenology, and foodweb structure. Climate models have simulated changes in physical ocean properties, including increased vertical stratification (Sarmiento *et al.*, 2004) and large-scale weakening (Vecchi *et al.*, 2006) and poleward shift (Yin, 2005) in northern hemisphere westerlies, in response to various future CO<sub>2</sub> emission scenarios. However, linking those changes directly to ecosystem effects has been difficult, because of the lack of our ability to develop realistic ecosystem models that then can be coupled with climate models. However, several approaches have been used to gain insight into ecosystem changes that result from global warming. In one early approach, physical variables from climate models were used to define biomes and their spatial trends, as well as a statistical model to project biological changes within the biomes (Sarmiento *et al.*, 2004). Ensembles of fully coupled biogeochemical models have also been applied to project phytoplankton changes in the 21st century (Henson *et al.*, 2010; Steinacher *et al.*, 2010). To interpret changes for living marine resources

(LMR) more directly, a spatial tuna ecosystem model (Sepodym) for bigeye tuna was driven with temperature and primary production from a climate model to forecast changes in abundance and distribution (Lehodey *et al.*, 2010). A second LMR approach used climate models to project future temperature changes and a bioclimate envelope model to forecast how 1066 marine species distributions and the resulting marine biodiversity will change with respect to temperature changes (Cheung *et al.*, 2009).

In this paper, we describe future North Pacific ecosystem changes over the 21st century with a climate model that includes a fully coupled ocean biogeochemistry model. Our approach uses the model output to define broad biomes, geographic regions that support a common ecosystem, then infer ecosystem changes based on the model-derived biological changes within and between these biomes. Our use of dynamic biomes follows that of Sarmiento *et al.* (2004), except that instead of defining the biomes with physical variables, we use biological variables from the climate model. A recent example using a biological variable to construct biomes identified six global biomes corresponding to various ranges of SeaWiFS surface chlorophyll (Hardman-Mountford *et al.*, 2008). We then go on to interpret these changes in the context of LMR.

## Material and methods

### The model

The NOAA Geophysical Fluid Dynamics Laboratory (GFDL) prototype Earth System Model (ESM2.1) is based on the successful CM2.1 coupled climate model used in the IPCC 4th Assessment and is composed of separate atmosphere, ocean, sea ice, and land models that interact through an online flux coupler (Delworth *et al.*, 2006). The ocean model has a resolution of  $1^\circ$  in latitude and longitude north of  $30^\circ\text{N}$ , whereas south of  $30^\circ\text{N}$  the latitudinal resolution progressively becomes higher, reaching  $1/3^\circ$  at the equator. A biogeochemical model [Tracers of Phytoplankton with Allometric Zooplankton (TOPAZ)] is integrated into the ocean model. TOPAZ includes all major nutrient elements (N, P, Si, and Fe) and four classes of phytoplankton: three classes of large phytoplankton ( $>5\ \mu\text{m}$  diameter) (i) diatoms, (ii) diazotrophs (nitrogen fixers), and (iii) all others, and a single class of small ( $<5\ \mu\text{m}$ ) phytoplankton (cyanobacteria and picoeukaryotes). Growth rates are modelled as a function of variable chlorophyll:carbon (C) ratios and are co-limited by nutrients and light. Photoacclimation is based on the Geider *et al.* (1997) algorithm, extended to account for co-limitation by multiple nutrients and including a parametrization for the role of iron in phytoplankton physiology. Loss terms include zooplankton grazing and ballast-driven particle export. Remineralization of detritus and cycling of dissolved organic matter are also explicitly included (Dunne *et al.*, 2005). Run in a historical mode in the North Atlantic, TOPAZ has been demonstrated to reproduce phytoplankton bloom dynamics in the SeaWiFS time-series, as well as the interannual variability over the 50-year Continuous Plankton Recorder period, but has not captured fully the regime shifts observed in that series (Henson *et al.*, 2009a, b). In the North Pacific, TOPAZ captures the magnitude of the north–south phytoplankton gradient fairly well, but the latitudinal location of the gradient region from subpolar to subtropical is shifted south, because of a coupled ocean atmosphere response as the ocean attempts to compensate for an overly cold northern polar region by fluxing heat to the atmosphere with associated deep winter convection. The latter tends to shift the subtropical gyre boundary to the south in the western and central basins (Ryckaczewski and Dunne, 2010).

The TOPAZ model was incorporated in the coupled climate simulations with biogeochemical parameters initialized from observations from the World Ocean Atlas 2001 (Conkright and Boyer, 2002) and Carbon Dioxide Information Analysis Center (Key *et al.*, 2004). The coupled climate model was spun up for 1000 years, with a fixed  $\text{CO}_2$  atmospheric boundary condition of 286 ppm. For an additional 100 years, the atmospheric boundary condition was switched to a fully interactive atmospheric  $\text{CO}_2$  tracer. Simulations were then made based on the  $\text{CO}_2$  trajectory described by the A2 scenario from the IPCC Special Report on Emission Scenarios (SRES; Nakićenović *et al.*, 2000), where atmospheric  $\text{CO}_2$  increases continuously from  $\sim 370$  ppm in 2000 to 850 ppm in 2100.

We focus on changes in the oceanic North Pacific, so use the domain from the equator to the northern boundary of the Subarctic Gyre, which includes the Gulf of Alaska, but not the Bering Sea or the Sea of Okhotsk. We use monthly model output from 1998 to 2100 covering the North Pacific from  $120^\circ\text{E}$  to  $78^\circ\text{W}$  and from  $0^\circ$  to the northern boundary of the Subarctic Gyre (Figure 1) in this analysis. Primarily, we use three

depth-integrated, biological variables, integrated from 0 to 200 m, in our analysis: phytoplankton biomass, primary production, and proportion of large phytoplankton. Modelled sea surface temperature (SST) and surface nitrate are also used in the analysis.

### Extension to fish catches

To extend the model results of changes in biome areas and biome primary production to potential fisheries impacts, we take an empirical approach. In particular, once we have determined our biomes, we estimate fish catch at the beginning of the century in each biome from the annual commercial fisheries catches summed over all species, gears, and countries, from four broad oceanic regions in the North Pacific (northeast Pacific, northwest Pacific, eastern central Pacific, and western central Pacific) provided in the Sea Around Us website ([www.seaaroundus.org](http://www.seaaroundus.org)). We use the average annual catch over the period 1997–2006 as the baseline catch within each region for year 2000. Then, to estimate the biome catch for any year  $t$ , we multiply the biome catch for 2000 by the ratio of total biome primary production in year  $t$  divided by the total biome primary production in year 2000. This estimate assumes that the biome catch varies proportionally with biome area and mean biome primary production. There is empirical evidence of the latter relationship both between ecosystems (Iverson, 1990) and within ecosystems (Ware and Thomson, 2005). Although we report the biome catches, it is the relative differences in catch per unit area (CPUA) between the various biomes used in projecting the effect to overall North Pacific catches from the replacement of one unit of area of one biome by another biome. This assumes that the biome CPUA computed comes from regional catches based on comparable levels of fishery exploitation. This seems reasonable, because the catches are derived from broad oceanic areas and are averaged over the same 10-year period.

### Results

The spatial distribution of the model 20-year mean of the total (large plus small) phytoplankton density integrated to the bottom of the euphotic zone displays three broad regions: a region of high phytoplankton density along the equatorial upwelling (EU) region, a region of high density generally north of  $30^\circ\text{N}$ , and a third region of low density in the subtropical gyre (Figure 1a). A frequency distribution of North Pacific modelled depth-integrated phytoplankton density exhibits a bimodal distribution with peaks at  $\sim 1$  and  $1.75\ \text{g C m}^{-2}$  and a trough between these peaks ranging from  $1.3$  to  $1.6\ \text{g C m}^{-2}$ . Therefore, based on the phytoplankton density distribution, there is a natural separation between regions with densities that exceed the  $1.3$ – $1.6\ \text{g C m}^{-2}$  range and those with densities less than that range. Within this  $1.3$ – $1.6\ \text{g C m}^{-2}$  range, all values partition the North Pacific into three contiguous regions. A value of  $1.35\ \text{g C m}^{-2}$  was selected to define the biomes, because the biome boundaries defined with this density value appear to generate the biome boundaries most consistent with patterns observed from SeaWiFS surface chlorophyll (Figure 1b). Specifically, using a value of  $1.35\ \text{g C m}^{-2}$ , we define the EU biome as the area south of  $20^\circ\text{N}$ , with annual average depth-integrated total phytoplankton density  $\geq 1.35\ \text{g C m}^{-2}$ . The large area north and west of the EU, with phytoplankton density  $< 1.35\ \text{g C m}^{-2}$ , corresponds closely to the subtropical gyre and it is hence termed the subtropical biome. The region north of the subtropical biome, with

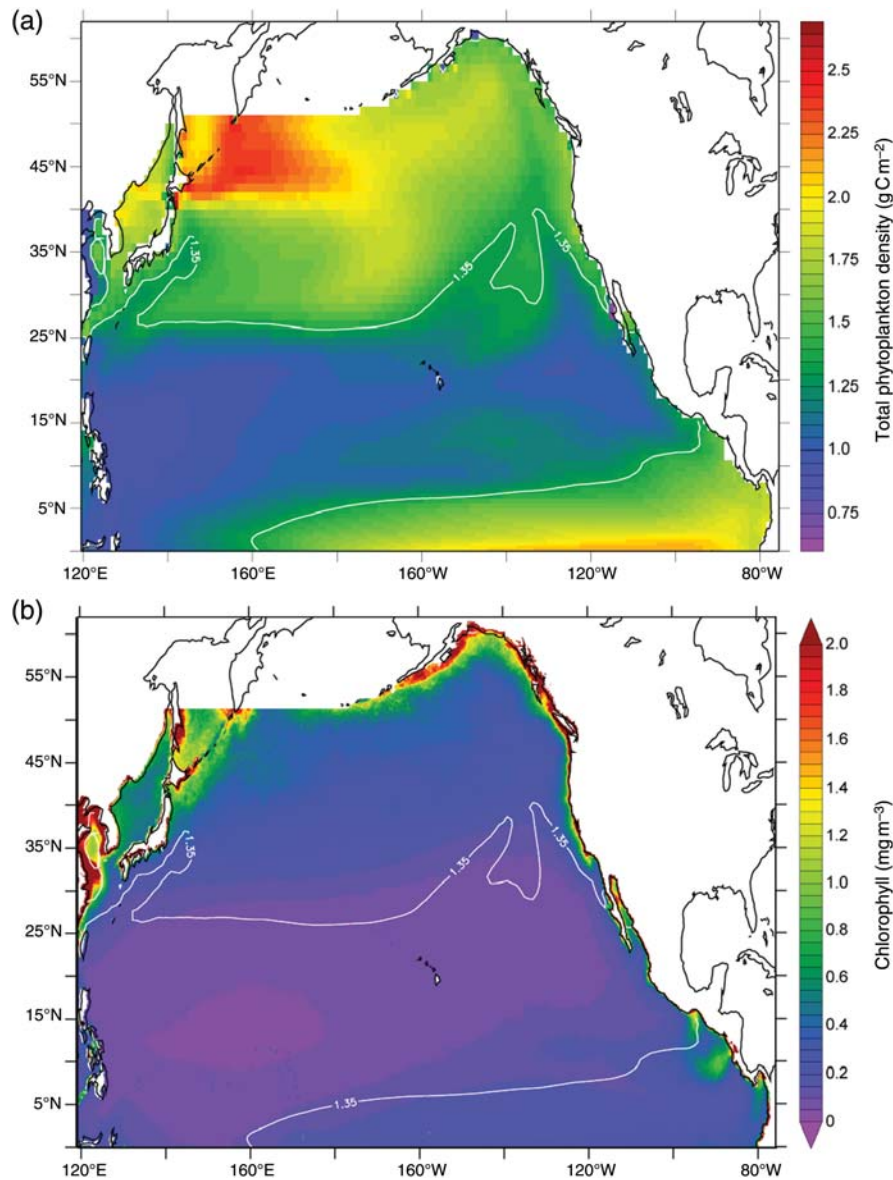


**Figure 1.** (a) Mean depth-integrated total phytoplankton, 1998–2017, with the model subtropical biome boundary ( $1.35 \text{ g C m}^{-2} \text{ d}^{-1}$ ) as the white line. (b) Mean SeaWiFS surface chlorophyll density, 1998–2007, with the model subtropical biome boundary as the white line.

phytoplankton density  $\geq 1.35 \text{ g C m}^{-2}$ , reaching northwards to the northern limit of the Subarctic Gyre and including the Transition Zone, is termed the temperate biome (Figure 1a).

Although the SeaWiFS data estimate surface chlorophyll and not the model's depth-integrated phytoplankton, the SeaWiFS data do capture the EU area with high chlorophyll, the subtropical gyre with low chlorophyll, and the Transition Zone and Subarctic Gyre regions of high surface chlorophyll (Figure 1b). An overlay of the model biome boundaries indicated as  $1.35 \text{ g C m}^{-2}$  contour lines over the mean surface chlorophyll annual climatology from SeaWiFS surface chlorophyll density reveals general correspondence between the regions of high and low surface chlorophyll and the model biome boundaries (Figure 1b). The match is not perfect; the model boundary between the subtropical and the temperate biomes lies farther south, in the centre of the basin, and displays more latitudinal variation at the east and west sides of the basin than suggested by SeaWiFS data (Figure 1b). The differing

geographical expression of these biomes between the model and the SeaWiFS chlorophyll are largely because of physical biases in the gyre circulation patterns common in this class of climate model, as demonstrated by Yin (2005). For example, the differences persist even if we were to increase the level of phytoplankton density that defines the boundary between the subtropical and the temperate biomes say to  $1.5$  or  $1.6 \text{ g C m}^{-2}$ . To fit better the pattern of SeaWiFS data in the central region, the contour line would shift north only slightly in the centre, whereas the east and west ends would shift north by  $5^\circ$  of latitude, or more, and the overall fit to the SeaWiFS pattern would not be as good as it is with  $1.35 \text{ g C m}^{-2}$ . We also considered using other variables, including nitrate, proportion of large phytoplankton, and primary production to define biomes, but these all replicated closely the spatial pattern of our three phytoplankton-based biomes.

Based on our phytoplankton-derived biome boundaries, we estimate the area of each biome annually from the model

depth-integrated phytoplankton data. A time-series of the annual area of each biome reveals that the area of the subtropical biome expands linearly from  $\sim 41$  million  $\text{km}^2$  in 2000 to  $\sim 50$  million  $\text{km}^2$  in 2100, an increase of 29.5% per 100 years (Figure 2a, Table 1). The areas of the temperate and EU biomes contract linearly, resulting in declines of 34 and 27.7% per 100 years, respectively (Figure 2a, Table 1). This pattern is largely invariant of the

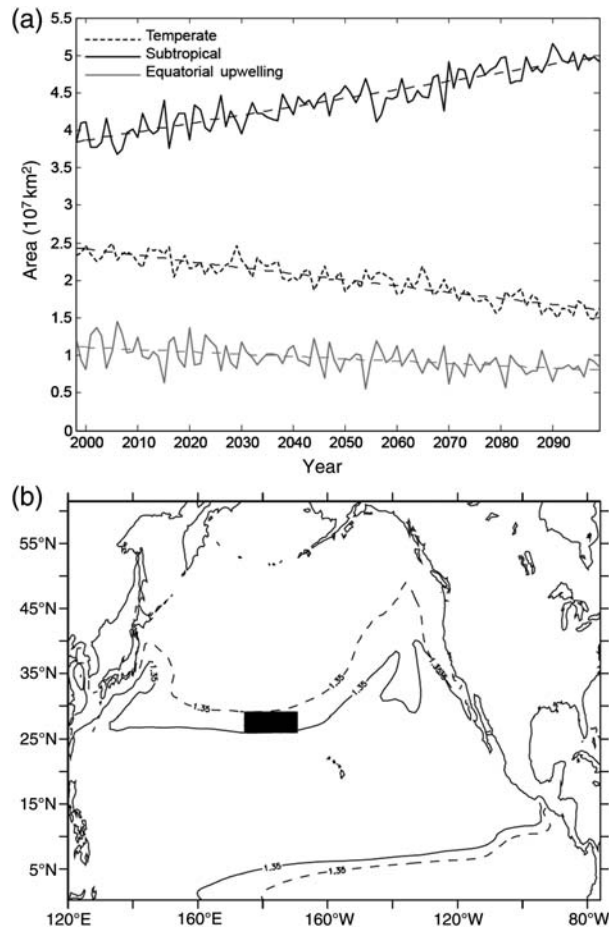


**Figure 2.** (a) Time-series of the annual area of the subtropical, temperate, and EU biomes, 1998–2100. (b) Boundary of the subtropical biome; black line represents mean position over 1998–2017 and dashed line represents mean position over 2080–2099. The black box is the area over which chemical and biological time-series are computed in Figure 3.

**Table 1.** Percentage change over 100 years of physical and biological variables for each biome and the total North Pacific, 1998–2100.

Parameter	Temperate	Subtropical	EU	North Pacific
Area	−34.0	29.5	−27.7	−
Mean PP	−5.5	−2.4	17.1	−4.3
Total biome PP	−37.7	26.4	−15.1	−4.3
Fish catch	−37.7	26.4	−15.1	−7.3
Phytoplankton biomass	−8.0	−7.6	−5.2	−13.4
% Large	−12.1	−7.3	−10.0	−26.9
SST	4.7	7.7	9.6	13.5

PP, primary production; SST, sea surface temperature.

specific phytoplankton density level we use to define the biome boundary. For example, if we use a value of  $1.5 \text{ g C m}^{-2}$  to define the subtropical boundary, the subtropical biome is larger and increases at a slightly lower rate of 26% per 100 years, whereas the EU and the temperate biomes are smaller and decrease at higher rates of 34 and 46% per 100 years, respectively.

A map with contours of the 20-year mean position of the subtropical boundary at the beginning and the end of the 21st century demonstrates that the subtropical–temperate boundary shifts northwards generally  $\sim 5$ – $10^\circ$  of latitude, whereas the subtropical–EU boundary shifts a few degrees south and contracts eastwards at the equator by  $\sim 20^\circ$  of longitude (Figure 2b). The expansion of the subtropical biome, by our definition, occurs as annual phytoplankton densities fall below the defined level of  $1.35 \text{ g C m}^{-2}$ . However, in regions where the subtropical biome expands, we observe concurrent changes in many other physical, chemical, and biological variables, indicating that our phytoplankton-based biome definition serves as a proxy for changes in a suite of variables. We observe this, for example, when we take a box located in the temperate biome at the beginning of the century and the subtropical biome at the end of the century and construct time-series of annual values of maximum surface nitrate, mean depth-integrated primary production, mean depth-integrated phytoplankton density, and the mean proportion of large phytoplankton all averaged over the area of the box (Figure 2b). All time-series reveal substantial concurrent declines, several exceeding 50% (Figure 3). Furthermore, these time-series reveal that variables at edges of dynamic biome boundaries exhibit large temporal changes and, hence, these locations are excellent sites for monitoring climate change effects (Figure 3). In addition to changes in annual values, the seasonality can change as the biomes switch. For example, the 20-year median, monthly depth-integrated primary production estimates in the boundary box at the beginning and the end of the century reveal the temperate seasonality, with a spring peak at the beginning of the century that is replaced by a subtropical, less seasonally variable, pattern at the end of the century (Figure 4).

The mean annual primary production in each of the three biomes changes linearly over the century, declining by 5.5 and 2.4% per 100 years in the temperate and the subtropical biomes, respectively, but increasing by 17.1% per 100 years in the EU biome (Table 1). Total biome annual primary production, computed by multiplying the annual biome primary production by the annual biome area, indicates a decrease in the temperate and the EU biomes of 37.7 and 15.1% per 100 years, respectively, whereas the subtropical biome primary production increases by 26.4% per 100 years (Table 1, Figure 5a). In 2000, the total subtropical biome primary production accounts for  $\sim 45\%$  of North Pacific primary production, whereas the temperate and EU biomes each accounts for  $\sim 31$  and 24%, respectively (Figure 5a). By 2100, the total subtropical biome primary production accounts for  $\sim 50\%$  of the North Pacific primary production, whereas the temperate and EU biomes each account for  $\sim 20$  and 30%, respectively (Figure 5a).

To estimate the potential effect from the changes in biome area and biome primary production on fish catches, we begin with estimates of total fish catch and areas for four high seas regions, the northeast Pacific, northwest Pacific, west central Pacific, and east central Pacific from the Sea Around Us website ([www.seaaroundus.org](http://www.seaaroundus.org)). Our temperate biome spans the northeast and the northwest Pacific regions. Hence, for the temperate biome,

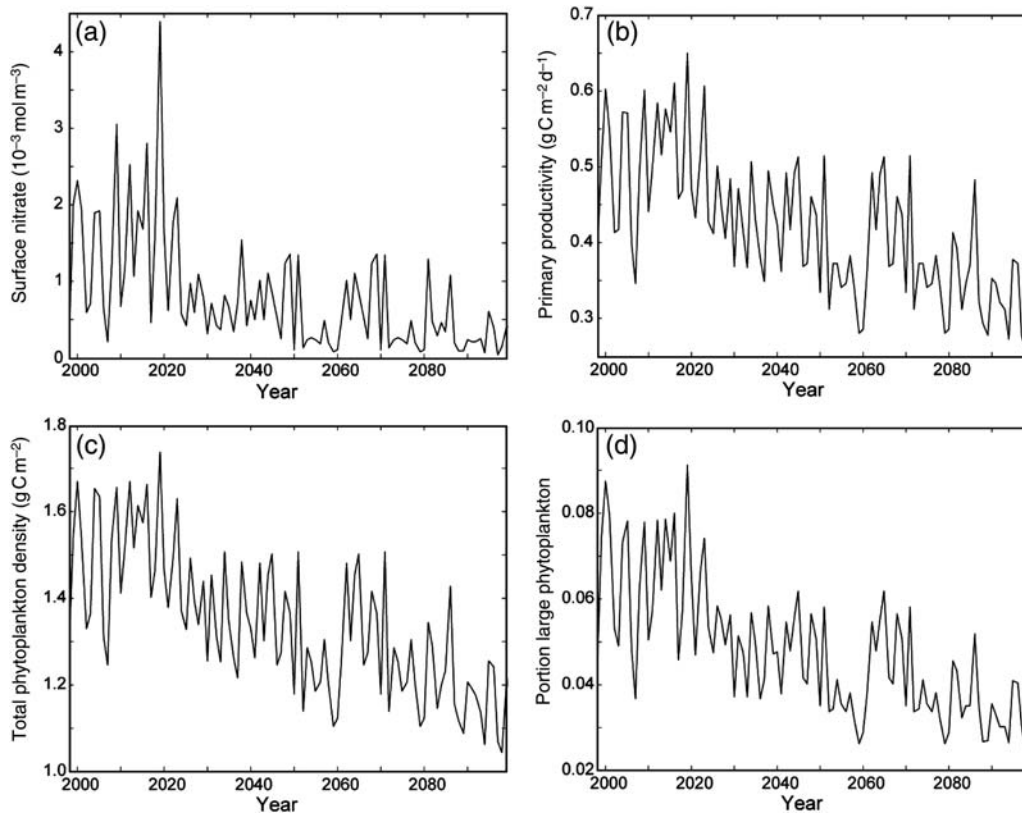


**Figure 3.** Time-series, 1998–2100, of chemical and biological variables averaged over a box, 27–29°N latitude, 175°E–170°W longitude, located in the temperate biome at the beginning of the century and the subtropical biome at the end of the century. (a) Maximum annual surface nitrate, and annual mean: (b) depth-integrated annual primary production, (c) depth-integrated total phytoplankton density, and (d) depth-integrated proportion of large phytoplankton.

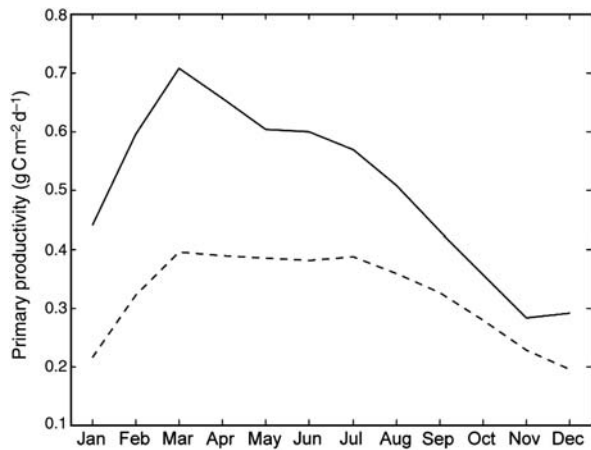


**Figure 4.** Median monthly depth-integrated primary production averaged over the box, 27–29°N latitude, 175°E–170°W longitude, located in the temperate biome at the beginning of the century and the subtropical biome at the end of the century. The solid line is the 1998–2017 median; the dashed line is the 2080–2099 median.

we estimate a CPUA for 2000 of  $0.13 \text{ t km}^{-2}$ , computed as the total catch of the northwest and the northeast regions averaged over the 1997–2006 period and divided by their combined area. Our subtropical biome spans the west central and the east central Pacific regions. Therefore, for this biome, we estimate a CPUA of  $0.08 \text{ t km}^{-2}$  for 2000, computed as the total catch of

the west and the east central Pacific regions averaged over the 1997–2006 period and divided by their combined area. Our EU biome also extends into both the east and the west central Pacific regions; we therefore use the same estimate of CPUA of  $0.08 \text{ t km}^{-2}$  for 2000 for this biome as well. Hence, we estimate the EU and the subtropical biomes per unit area produce  $\sim 62\%$  of the temperate biome fish CPUA. We expand the biome-specific CPUAs for 2000 to biome catches for 2000 by multiplying by the biome areas. The biome catch for year  $t$  is computed as the biome catch for 2000 multiplied by the ratio of total biome primary production for year  $t$  divided by total biome primary production for 2000. The fish catch in the subtropical biome is estimated to increase by  $\sim 26\%$  over the century, going from  $\sim 3.0$  to  $\sim 3.8$  million tonnes (Table 1, Figure 5b). The fish catch within the temperate biome is projected to decline by  $\sim 38\%$  from  $\sim 3.1$  to 1.9 million tonnes, whereas catches in the EU biomes are estimated to decline by  $\sim 15\%$  over the century, from  $\sim 0.9$  to 0.76 million tonnes (Table 1, Figure 5b). The within-biome percentage changes in fish catches are the same as the percentage change for total biome primary production, because within each biome, fish catch is a constant fraction of total biome primary production (biome area multiplied by mean biome primary production). However, the total North Pacific fish catch is projected to decline by 7.3%, slightly more than the 4.3% decline in North Pacific primary production, because  $8.3 \text{ million km}^2$  of the temperate biome area with the higher CPUA is replaced by a subtropical biome with a 62% lower CPUA (Table 1, Figure 5b). Both

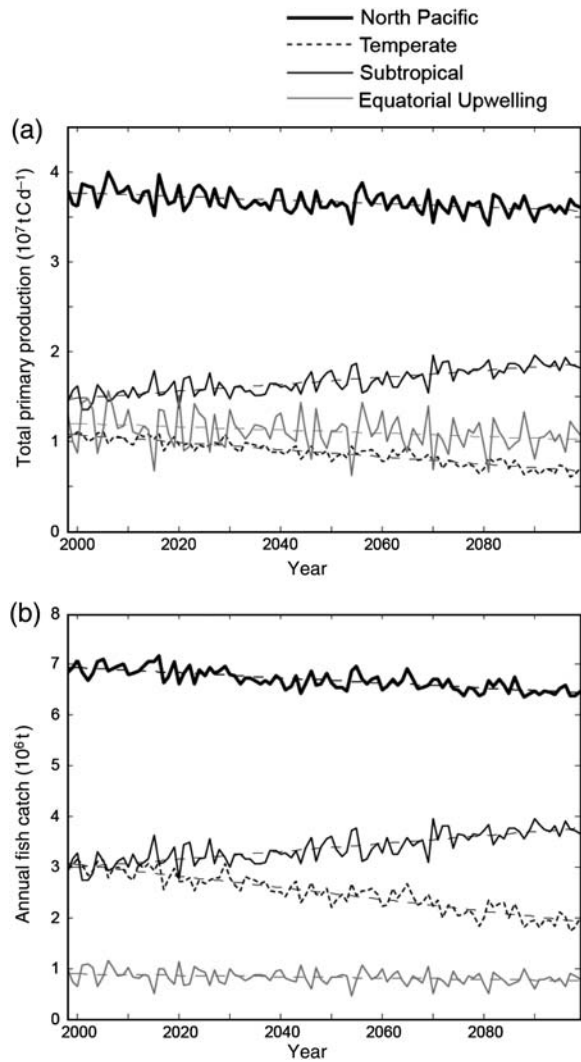


**Figure 5.** Time-series, 1998–2100, of (a) depth-integrated total primary production, (b) annual fish catch for the total North Pacific, temperate, subtropical, and EU biomes.

the subtropical and the EU biomes increase their contributions to the total North Pacific catches over the century from  $\sim 46$  and 9%, respectively, at the beginning to 56 and 12%, respectively, by the end (Figure 5b). The temperate biome's contribution to total North Pacific fish catch declines over the century from 45 to 31% (Figure 5b).

For a number of physical and biological variables, based on the dynamic nature of the biomes, their within-biome means change less than their means computed over the entire North Pacific. For example, mean annual phytoplankton densities exhibit linear declines of  $\sim 5.2$ , 7.6, and 8.0% per 100 years for the EU, subtropical, and temperate biomes, respectively, whereas for the entire North Pacific, the decline is 13.4% per 100 years (Table 1). The proportion of large phytoplankton to total phytoplankton density declines 10.0, 7.3, and 12.1% per 100 years for the EU, subtropical, and temperate biomes, respectively, whereas for the North Pacific, the decline is 26.9% per 100 years (Table 1). SST increases within each biome by 9.6, 7.7, and 4.7% per 100 years, for the EU, subtropical, and temperate biomes,

**Table 2.** Mean density ( $\text{g C m}^{-2}$ ) of depth-integrated diazotrophs, diatoms, and other large phytoplankton in each biome over 20-year periods at the beginning and end of the century.

Biome and period	Diazotrophs	Diatoms	Others
Temp 1998–2017	0.0612	0.1439	0.1101
Temp 2080–2099	0.0511	0.1171	0.0911
ST 1998–2017	0.0374	0.0139	0.0235
ST 2080–2099	0.0310	0.0136	0.0189
EU 1998–2017	0.1075	0.1397	0.2171
EU 2080–2099	0.1015	0.1269	0.1902

Temp, temperate; ST, subtropical.

respectively, whereas for the entire North Pacific, the increase is 13.5% per 100 years (Table 1).

The change in composition of the large phytoplankton community over the 21st century appears modest in all biomes. The 20-year mean densities of diazotrophs, diatoms, and other large phytoplankton are all lower, but in roughly the same proportion at the end of the century compared with the beginning in both the temperate and the EU biomes (Table 2). The subtropical biome diatom density, although at very low level, remains essentially unchanged over the century, whereas the density of both diazotrophs and others decline slightly (Table 2).

Although the change in mean annual primary production in the subtropical biome is a very modest decrease of 2.4% per 100 years, this small average change results from increases at both the upper and the lower tails of the productivity frequency distribution. Specifically, the least productive waters, those with primary production  $< 0.3 \text{ g C m}^{-2} \text{ d}^{-1}$  largely in the centre of the subtropical biome, increase from  $\sim 11$  to  $\sim 26$  million  $\text{km}^2$  or  $\sim 91.9\%$  per 100 years (Figure 6a–c). However, the most productive subtropical waters, those with annual primary productivity  $\geq 0.6 \text{ g C m}^{-2} \text{ d}^{-1}$  around the edge of the biome, also increase from  $\sim 3.1$  to  $\sim 4.6$  million  $\text{km}^2$  or  $\sim 72.3\%$  per 100 years. For the EU biome, the 17% per 100 years increase in mean annual primary production is largely because of a 88.8% per 100 years increase in the area of its most productive waters next to the equator, those  $\geq 1.2 \text{ g C m}^{-2} \text{ d}^{-1}$  (Figure 6a–c). The time-series of the annual area of highly productive EU waters displays pronounced interannual variation, likely the influence of ENSO (*El Niño* Southern Oscillation) events, whereas the increase in the area of the least productive subtropical waters exhibits some suggestion of decadal variation (Figure 6c). For the temperate biome, the decline in primary production occurred reasonably uniformly across its range of primary production.

The change in SST (sea surface temperature) over the North Pacific is examined with overlays of the 10, 20, and 30°C SST isotherms computed from 20-year means from the beginning and the end of the century (Figure 7a). The 10 and 20°C isotherms shift northwards by  $\sim 5^\circ$  of latitude over the century (Figure 7a). There is no 30°C isotherm observed at the beginning of the century, whereas a large area with SSTs equal to or exceeding 30°C appears by the end of the century. In the subtropical and the EU biomes, 40–60% of area with SST between 25 and 30°C is replaced by area with SST equal to or exceeding 30°C. In the subtropical and the EU biomes, by the end of the century, there are more than 25 million  $\text{km}^2$  of water with a mean SST of  $> 31^\circ\text{C}$ , whereas there was virtually none at the beginning of the century (Figure 7b).

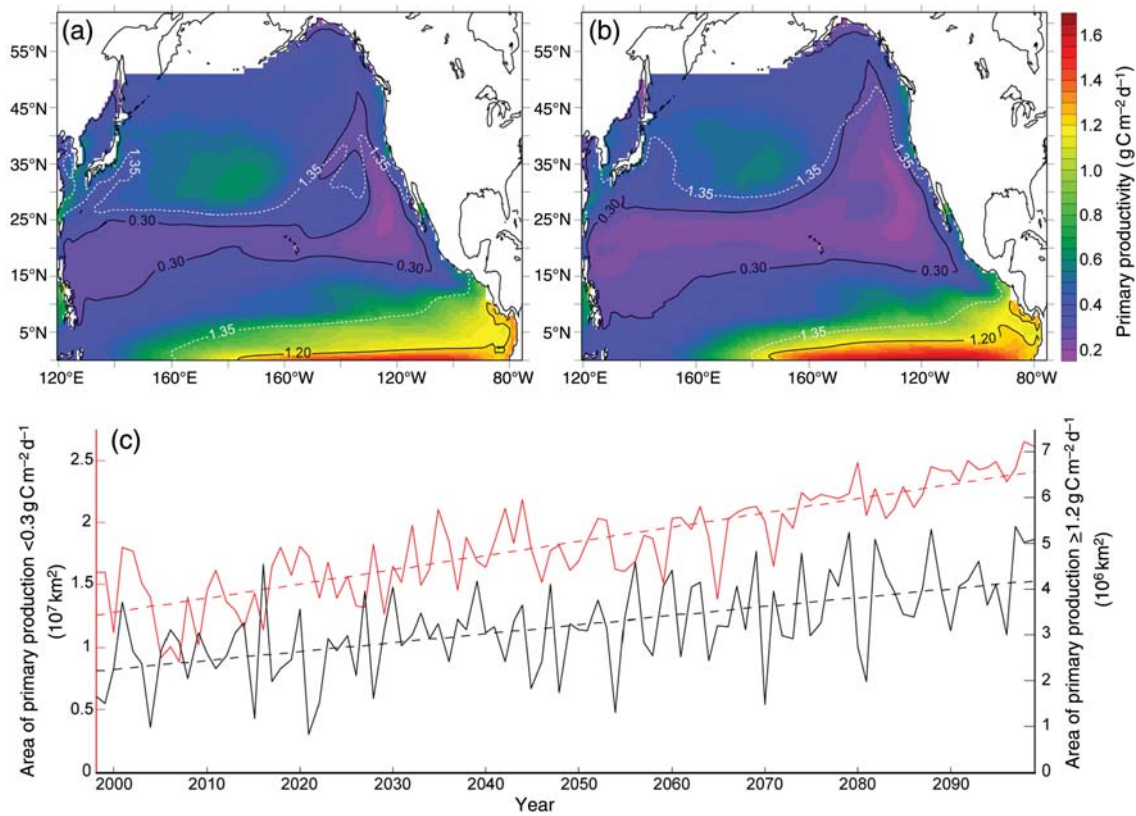


**Figure 6.** Mean depth-integrated primary production, (a) 1998–2017, (b) 2080–2099, (c) time-series of the area with primary production  $< 0.3 \text{ g C m}^{-2} \text{ d}^{-1}$  in the subtropical biome (red line) and the time-series of the area with production  $\geq 1.2 \text{ g C m}^{-2} \text{ d}^{-1}$  in the EU biome. Dashed white lines in (a) and (b) indicate the biome boundaries.

## Discussion

### Overall biome changes

We use model output to divide the North Pacific, from the equator to the northern boundary of the Subarctic Gyre, into three broad biologically based biomes: EU, subtropical, and temperate. Although we define our biomes based on phytoplankton density, changes in the biome boundaries are associated with changes in a suite of physical, chemical, and biological variables. These biomes do represent areas with different physical forcing and biological properties. The EU biome is exposed to near-continual upwelling, resulting in strong and persistent horizontal and vertical temperature gradients, relatively high primary production, and phytoplankton density with a moderate proportion of large phytoplankton. Interannual dynamics are strongly driven by ENSO dynamics. The subtropical biome represents the subtropical gyre and is characterized by a weak seasonal cycle, warm, vertically stratified water, low primary production, and low phytoplankton density composed almost entirely of small phytoplankton. The temperate biome contains the Subarctic Gyre and the Transition Zone, characterized by a strong seasonal cycle with deep winter vertical mixing, relatively high primary production, and phytoplankton density with a moderate proportion of large phytoplankton. These biomes correspond closely to biomes determined using other approaches. For example, our subtropical and temperate biomes compare with Longhurst’s (1998) trade wind and westerly wind biomes and the permanently stratified subtropical and polar biomes of Sarmiento *et al.* (2004).

The expansion of the subtropical biome and the contraction of the EU and temperate biomes represent key North Pacific responses to global warming. By the end of the 21st century, the GFDL earth system model driven by the IPCC SRES A2 scenario projects the subtropical biome to become 30% larger and the temperate and EU biomes 34 and 28% smaller than at the beginning of the century. These biome changes are consistent with results from other climate model studies, revealing large-scale weakening (Vecchi *et al.*, 2006) and poleward shift (Yin, 2005) in northern hemisphere westerlies and basin-scale decreases in the magnitude of vertical velocities in both the temperate and the subtropical biomes (Ryckaczewski and Dunne, 2010). The changes in biome areas account for much of the 13% decline in phytoplankton biomass and the 27% decline in the proportion of large phytoplankton over the century for the entire North Pacific, based on the replacement of large areas of high phytoplankton density water, containing more large phytoplankton, by water with low phytoplankton density and a small proportion of large phytoplankton. Overall, total primary production in our North Pacific domain declines by a very modest 4.3% per 100 years, which, by itself, does not convey the nature of the change observed from the biome approach. The increased primary production observed in the EU biome is largely a response of the increased phytoplankton growth, the result of warming there.

The change in the biome area and production suggests that the potential future  $\text{CO}_2$  increase may have the most negative impact on the temperate biome ecosystem. Total primary production is

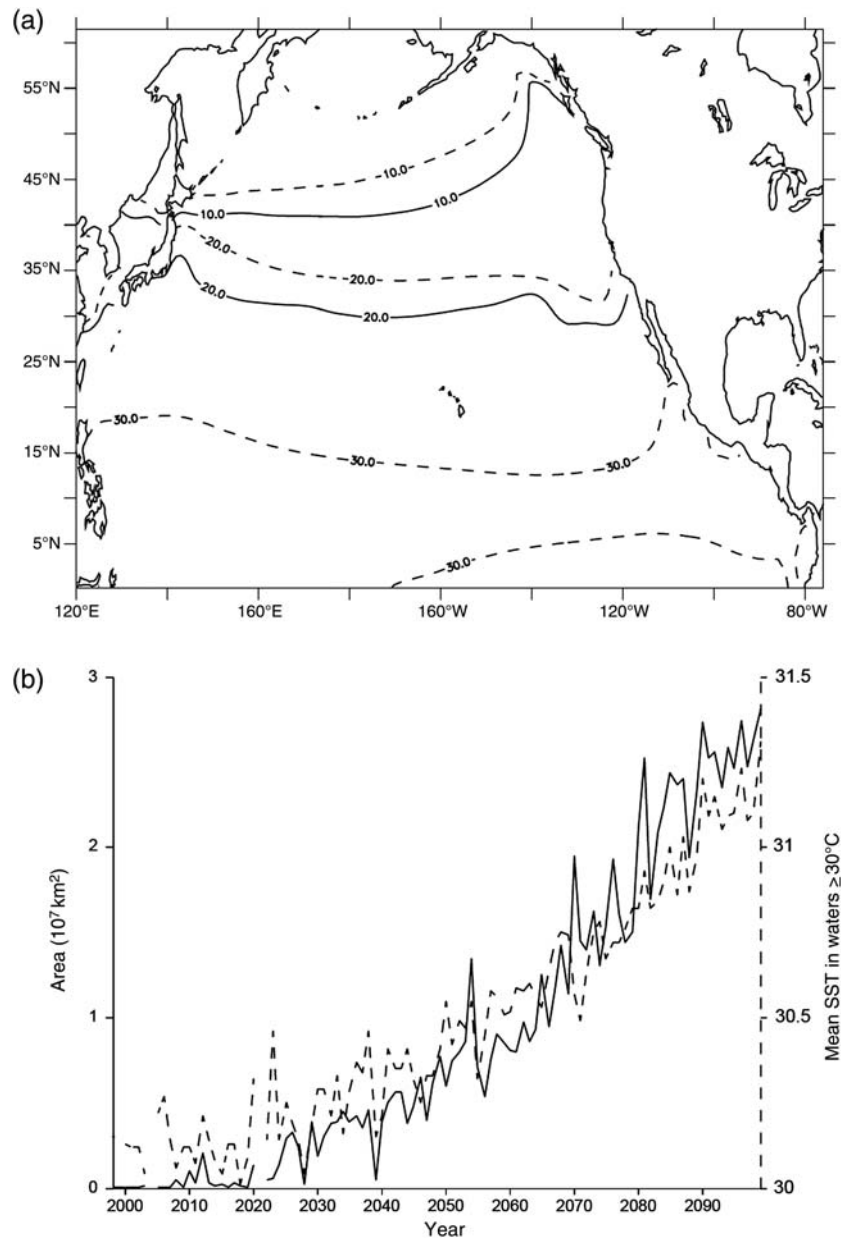


**Figure 7.** (a) Mean SST contours, 1998–2017 indicated in black, 2080–2099 indicated as dashed line. (b) Annual area (black) and mean SST (dashed) for water with  $SST \geq 30^{\circ}C$ .

projected to decline by  $\sim 38\%$  per 100 years and have a positive effect on the subtropical biome ecosystem, which is projected to increase in area by  $\sim 30\%$  and in total biome primary production by  $\sim 26\%$  per 100 years.

### Implications for living marine resources

Overall, the total North Pacific fish catches are projected to decline by  $\sim 7\%$  over the century, compared with approximately a 4% decline in primary production. The 7% decline incorporates both the decline in primary production and the replacement of 8.3 million  $km^2$  of temperate habitat with subtropical habitat, which is estimated, based on empirical fish catches, to produce only 62% of the temperate fish catch. Therefore, from the perspective of the total North Pacific, fish catches are projected to decline only modestly over the century. Although in the face of rising

demand for fish, this might mean additional pressures from overfishing.

However, from a biome perspective, things look very different. The temperate biome supports many protected species, including seabirds and marine mammals, as well as species that are important to fisheries, including salmon, pomfret, albacore, bluefin tuna, swordfish, and squid. The reduction by more than one-third in the carrying capacity of this biome and its fish catches will raise severe challenges for resource managers, who will have to cut fishing effort and quotas substantially to respond to this slow long-term declining trend. Some species might be able to move northwards into the Bering Sea or Arctic waters, but that would involve changes in migration patterns and adaptation to new ecosystems. Many species, including salmon, squid, albacore, bluefin tuna, swordfish, and tropical seabirds that use the temperate biome as

foraging habitat will find this foraging habitat reduced by one-third. Moreover, these same species have spawning or nesting habitat well to the south in low latitudes linked to equatorial or other regional oceanographic processes, or for salmon to specific streams, and for tropical seabirds to specific subtropical islands. These animals, especially their juveniles, might be constrained by the distance between their spawning habitats and their foraging habitats and could incur greater migration costs if the adults forage in far northern waters. This could especially affect tropical seabirds that make very frequent forage migrations to temperate habitat to provide food for their chicks on subtropical islands. In the Northeast Pacific, the temperate–subtropical biome boundary moves north  $\sim 1000$  km per 100 years ( $10 \text{ km year}^{-1}$ ) resulting in a very significant northward contraction of the temperate biome. Species using this habitat, such as salmon migrating back to North American spawning streams, will either be compressed northwards and take a longer migration path or be forced to transit less productive subtropical waters.

In contrast, in the subtropical biome, whereas the mean primary production is forecast to decline slightly, the area is projected to increase by  $\sim 30\%$ , resulting in a 26% increase in primary production and fish catch. Many of the commercially important subtropical species, including the tropical tuna (skipjack, yellowfin, and bigeye), marlins, and fish such as mahi–mahi and moonfish, use both the expanding subtropical and the contracting EU biomes. When these two biomes are taken together, their combined total fish catches are projected to increase by 16.8% per 100 years. Although the least productive centre of the subtropical biome is expected to almost double over the century, the more productive perimeter region in the subtropical biome and the most productive area of EU biome will almost double as well. These latter habitats are important for foodwebs that reach the top trophic levels, because of their elevated phytoplankton density and primary production. Moreover, for the tropical tuna, their optimal spawning habitat is water with  $27\text{--}29^\circ\text{C}$  SST and, currently, a significant portion of the productive EU waters is too cold for spawning. The projected increase in SST in the EU biome and the increase in primary productivity will likely expand productive tropical tuna spawning habitat. The projected eastward expansion of the subtropical biome along the equator by 2000 km per 100 years will likely result in a similar eastward shift in the western Pacific skipjack purse-seine fishing grounds, with both positive and negative impacts on different island countries from changes in fishing access revenues.

### Uncertain role for new, extreme biomes

The area with mean annual SST  $\geq 30^\circ\text{C}$  is projected to increase from a negligible amount at the beginning of the century to  $>25$  million  $\text{km}^2$ , with a mean SST exceeding  $31^\circ\text{C}$  by the end of the century. Although historical distributions of species can be used as potentially useful indicators of future distributions, the ecosystem impact from the large increase in the area of SST exceeding  $30^\circ\text{C}$  in the subtropical and the EU biomes is difficult to forecast, because this is largely new thermal habitat and we do not know which species will adapt to it. However, species currently in the area affected by the elevated SST might be unable to remain in the new habitat based on a potential mismatch between the demand for oxygen and the capacity of oxygen supply to tissues that restricts fish tolerance of thermal extremes (Pörtner and Knust, 2007; Cheung *et al.*, 2009). Some of the high SST habitat in the western equatorial region will include the least

productive waters, whereas the eastern portion of this habitat will extend into the productive EU biome. This elevated SST exceeds the optimal spawning habitat for tropical tunas, but might still be suitable as less optimal spawning habitat.

### Implications for new emphases in monitoring

The biome approach identifies the edges of the shifting biome boundaries as areas with some of the greatest physical and biological changes and, hence, locations for monitoring. In particular, our results suggest one region to monitor is along the north subtropical biome boundary and especially at the eastern end of that boundary around  $140^\circ\text{W}$  longitude, where the boundary shifts northwards by more than 1000 km per 100 years. Another region is along the equator where the subtropical–EU boundary shifts eastwards by  $\sim 2000$  km per 100 years.

One of the most rapid rates of change observed with the model data is the expansion of the area of least productive waters within the subtropical biome, which is estimated to increase at almost 1% per year. This trend has already been observed over the past decade with SeaWiFS surface chlorophyll data, although the rate of expansion estimated from SeaWiFS data, some 2% per year for the North Pacific, is approximately twice the model estimate (Polovina *et al.*, 2008). The higher rate estimated with the 10-year SeaWiFS data might reflect both a decadal and longer time-trend, whereas the decadal trend is averaged out in the 100-year period, as recently demonstrated in the attribution study of Henson *et al.* (2010).

The area of our subtropical biome,  $\sim 39$  million  $\text{km}^2$ , is similar in size to the 42 million  $\text{km}^2$  subtropical gyre biome defined by physical variables in Sarmiento *et al.* (2004), but the latter was estimated to expand by only 4% by 2050, whereas we estimate approximately a 19% increase in area by 2050 and 30% by 2100. Key differences between our study and the Sarmiento *et al.* (2004) study are that they combined the results from four physical models and defined the subtropical biome with physical variables, whereas we use only one climate model that includes a phytoplankton model and uses a biological variable to define our subtropical biome. This highlights an important caveat regarding our work. We have used the output from only one climate model and it would be prudent to incorporate results from other climate models, before giving too much weight to these findings. A second caveat is that our focus is to examine how projected climate change will affect ecosystems of the large oceanic biomes. Although output from coastal ecosystems is included in our spatial averages, they account for such a small portion of the area relative to the oceanic regions that they do not have much influence on the results. Therefore, changes in coastal ecosystems should not be inferred from our oceanic results. For example, this same model analysed only for the region of the California Current ecosystem suggests increased primary production by the end of the century (Ryckaczewski and Dunne, 2010).

### Acknowledgements

We acknowledge Drs Charles Stock and Anand Gnanadesikan for their helpful discussions of the GFDL model output. We also wish to acknowledge the use of the Ferret program for analysis and graphics in this paper. Ferret is a product of NOAA's Pacific Marine Environmental Laboratory (information is available at <http://ferret.pmel.noaa.gov/Ferret/>).

## References

- Cheung, W. W. L., Lam, V. W. Y., Sarmiento, J. L., Kearney, K., Watson, R., and Pauly, D. 2009. Projecting global marine biodiversity impacts under climate change scenarios. *Fish and Fisheries*, 10: 235–251.
- Conkright, M. E., and Boyer, T. P. 2002. *World Ocean Atlas 2001: Objective Analyses, Data Statistics, and Figures*, CD-ROM Documentation. National Oceanographic Data Center, Silver Spring, MD. 17 pp.
- Delworth, T., Broccoli, A. J., Rosati, A., Stouffer, R., Balaji, V., Beesley, J. A., Cooke, W., et al. 2006. GFDL's CM2 global coupled climate models. Part I: formulation and simulation characteristics. *Journal of Climate*, 19: 643–674.
- Dunne, J. P., Armstrong, R. A., Gnanadesikan, A., and Sarmiento, J. L. 2005. Empirical and mechanistic models for the particle export ratio. *Global Biogeochemical Cycles*, 19: GB4026. doi: 10.1029/2004GB002390
- Geider, R. J., MacIntyre, H. L., and Kana, T. M. 1997. Dynamic model of phytoplankton growth and acclimation, responses of the balanced growth rate and the chlorophyll *a*: carbon ratio to light, nutrient-limitation and temperature. *Marine Ecology Progress Series*, 148: 187–200.
- Hardman-Mountford, N. J., Hirata, T., Richardson, K. A., and Aiken, J. 2008. An objective methodology for the classification of ecological pattern into biomes and provinces for the pelagic ocean. *Remote Sensing of the Environment*, 112: 3341–3352.
- Henson, S. A., Dunne, J. P., and Sarmiento, J. L. 2009a. Decadal variability in North Atlantic phytoplankton blooms. *Journal of Geophysical Research*, 114: C04013, doi:10.1029/2008JC005139
- Henson, S. A., Raitos, D., Dunne, J. P., and McQuatters-Gollop, A. 2009b. Decadal variability in biogeochemical models: comparison with a 50-year ocean colour dataset. *Geophysical Research Letters*, 36: L21601.
- Henson, S. A., Sarmiento, J. L., Dunne, J. P., Bopp, L., Lima, I., Doney, S. C., John, J., et al. 2010. Detection of anthropogenic climate change in satellite records of ocean chlorophyll and productivity. *Biogeosciences*, 7: 621–640.
- Iverson, R. L. 1990. Control of marine fish production. *Limnology and Oceanography*, 35: 1593–1604.
- Key, R. M., Kozyr, A., Sabine, C. L., Lee, K., Wanninkhof, R., Bullister, J. L., Feely, R. A., et al. 2004. A global ocean carbon climatology: Results from GLODAP. *Global Biogeochemical Cycles*, 8: GB4031.
- Lehodey, P., Senina, I., Sibert, J., Bopp, L., Calmettes, B., Hampton, J., and Murtugudde, R. 2010. Preliminary forecasts of Pacific bigeye tuna population trends under the A2 IPCC scenario. *Progress in Oceanography*, 86: 302–315.
- Longhurst, A. 1998. *Ecological Geography of the Sea*. Academic Press, San Diego. 398 pp.
- Nakićenović, N., Alcamo, J., Davis, G., de Vries, B., Fenhann, J., Gaffin, S., Gregory, K., et al. 2000. *IPCC Special Report on Emissions Scenarios*. Cambridge University Press, Cambridge, UK, and New York, USA. 599 pp.
- Polovina, J. J., Howell, E. A., and Abecassis, M. 2008. The ocean's least productive waters are expanding. *Geophysical Research Letters*, 35: L03618. doi:10.1029/2007GL031745
- Pörtner, H., and Knust, R. 2007. Climate change affects marine fishes through the oxygen limitation of thermal tolerance. *Science*, 315: 95–97.
- Rykczewski, R. R., and Dunne, J. P. 2010. Enhanced nutrient supply to the California Current Ecosystem with global warming and increased stratification in an earth system model. *Geophysical Research Letters*, 37: L21606. doi:10.1029/2010GL045019.
- Sarmiento, J. L., Slater, R., Barber, R., Bopp, L., Doney, S. C., Hirst, A. C., Kleypas, J., et al. 2004. Response of ocean ecosystems to climate warming. *Global Biogeochemical Cycles*, 18: GB3003. doi:10.1029/2003GB002134
- Steinacher, M., Joos, F., Frölicher, T. L., Bopp, L., Cadule, P., Cocco, V., Doney, S. C., et al. 2010. Projected 21st century decrease in marine productivity: a multi-model analysis. *Biogeosciences*, 7: 979–1005.
- Vecchi, G. A., Soden, B. J., Wittenberg, A. T., Held, I. M., Leetmaa, A., and Harrison, M. J. 2006. Weakening of tropical Pacific atmospheric circulation due to anthropogenic forcing. *Nature*, 441: 73–76.
- Ware, D. M., and Thomson, R. E. 2005. Bottom-up ecosystem trophic dynamics determine fish production in the Northeast Pacific. *Science*, 308: 1280–1284.
- Yin, H. 2005. A consistent poleward shift of the storm tracks in simulations of 21st century climate. *Geophysical Research Letters*, 32: L18701. doi:10.1029/2005GL023684